J. A. Smith
Tzeu Lie Lin
K. J. Ranson
College of Forestry and Natural Resources
Colorado State University
Fort Collins, CO 80523

The Lambertian Assumption and Landsat Data

The Lambertian assumption, for ponderosa pine, may be more valid when analysis is restricted to slopes of less than 25° and effective illumination angles of less than 45°.

Abstract: *Analysis of terrain geometric effects on the optical scattering properties of dense* Pinus ponderosa *forest as measured by the Landsat multispectral scanner has been performed. A mountainous study site in Colorado was utilized in which effective view angles between the surface normal vector and the zenith satellite sensor angle ranged between 10 and 45°. Effective illumination angles between the surface normal vector and the sun at image acquisition ranged between 30 and 80°.*

Seventy-six sample points of similar cover density and type were selected within the study site. Topographic slope, aspect, and calculated incidence and exitance angles were merged with the multispectral Landsat response for MSS bands 4, 5, 6, and 7. Regression analysis was applied to the data in order to fit a generalized photometric function. The slope of the regression line may be compared to the expected value for Lambertian scattering and a test of significance performed. At the 95 percent significance level, the Lambertian assumption for ponderosa pine Landsat responses was rejected.

Further analysis was performed to determine under what topographic slope and incidence angle conditions the Lambertian assumption may be more appropriate for our ponderosa pine pixels. It is shown that the Lambertian assumption may be more valid when analysis is restricted to slopes of less than 25° and effective illumination angles of less than 45°.

Finally, an application of a generalized photometric function is discussed regarding the topographic-induced Landsat radiance variations versus surface cover variations. These effects are estimated by a method outlined by Horn and Bachman (1978).

Introduction

The Landsat sensors have the capability of acquiring imagery over broad areas with short data acquisition times. Consequently, to a good approximation, the data are obtained under a constant, vertical sensor angle and constant solar illumination angle with respect to the local nadir. That is, the phase angle is constant. If the topography of the scene is flat, all surfaces or materials are also viewed at constant sensor and illumination angles. Effects of directional scattering behavior of the scene surfaces on classification are minimized.

In mountainous terrain, however, the local surface normal varies and, consequently, a wide range of effective view and illumination angles are obtained, even for a single Landsat image. In these cases, classification of the data is severely impaired (Hoffer, 1974). Several authors have tried various correction procedures to improve the results obtained. These can be broken down into

Photogrammetric Engineering and Remote Sensing,
Vol. 46, No. 9, September 1980, pp. 1183-1189.

basically empirical approaches which make no assumptions concerning the physical behavior of scene elements and those methods utilizing some assumed natural characteristics of the scene elements (Hart, 1978). Examples of the first approach include channel ratio methods as discussed by Crane (1971) and Vincent (1973). Struve *et al.* (1977) give a detailed example of the second approach in which they assume Lambertian scattering behavior of the scene elements. This is used to normalize the satellite readings according to the cosine of the effective illumination angle. Topographic slope and aspect for each scene element are required to calculate the effective incidence angle.

Our objectives for the study presented here were to make a rigorous evaluation of the Lambertian assumption for Landsat and to examine various recommended correction procedures. In addition, we examined under what conditions the Lambertian assumption may be more correct. We selected a Landsat image of a mountainous region in Colorado and employed a photometric function developed by Minnaert (1941) to test the Lambertian assumption. A range of effective view angles of 10 to 45 degrees and effective illumination angles of 30 to 80 degrees were present in the data. Analysis was restricted to ponderosa pine (*Pinus ponderosa*) scene elements of similar cover density.

Analytical Background

The radiance or scene brightness incident upon the entrance aperture of the Landsat multispectral scanner (MSS) consists of the surface radiance attenuated by atmospheric transmittance plus an additive atmospheric path radiance term. The surface radiance, in turn, is given by the reflected solar flux plus reflected diffuse sky irradiance. Finally, radiance is converted to digital Landsat counts by the response of the Landsat scanner for each wavelength band. For the analyses reported here we are interested in the relationship between Landsat radiance and the surface scattering properties. The atmospheric path radiance is independent of the surface response function and can be dropped from further consideration, other than as an additive noise term. We will also ignore reflected diffuse sky radiance. The physical reasoning for this approximation is as follows. During the time of the satellite overpass, the investigators measured the fraction of diffuse sky irradiance to total irradiance at a location near the study site (Oliver *et al.*, 1975). For a solar zenith sun angle of 33 degrees, the diffuse irradiance fraction was less than twelve percent for all four Landsat MSS bands. Because all of the scene picture elements (pixels) selected for analysis were in direct sunlight, i.e., pixels shadowed due to topography were excluded, the direct sunlight must account for nearly 90 percent of the surface radiance contributed.

We can thus write the following model for Landsat scene radiance, L, given in digital counts at an effective view angle, e, and effective solar incidence angle, i:

$$L(\lambda,e) \simeq C(\lambda)\left[\frac{1}{\pi}E_o(\lambda)\cos i\ \rho(e,i)\right]T(\lambda)$$

or

$$L(\lambda,e) = A(\lambda)\cos i\ \rho(e,i) + \epsilon(\lambda)$$

where

C = the Landsat scanner calibration factor,
E_o = surface solar irradiance at the time of the Landsat overpass,
ρ = the scene bidirectional reflectance factor,
T = the atmospheric transmittance,
A = a constant, equal to $1/\pi\ C\ E_0\ T$,
λ = the spectral wavelength, and
ϵ = the error term.

Figure 1 shows the geometrical relationships between the sun, the Landsat satellite, and an arbitrary surface element.

If

θ_n = surface normal zenith angle or slope of the terrain surface,
θ_s = solar zenith angle,
ϕ_n = surface azimuth or aspect angle,

and

ϕ_s = solar azimuth angle,

then, since the satellite has nearly a vertical view angle, the effective incidence angle, i, and exitance angle, e, measured from the surface normal are defined by

$$\cos i = \cos\theta_s\cos\theta_n + \sin\theta_s\sin\theta_n\cos(\phi_s - \phi_n)$$

and

$$\cos e = \cos\theta_n.$$

If the surface behaves as a Lambertian scatterer, the bidirectional reflectance factor is independent of incidence and exitance angles. That is, $\rho(\lambda,e,i) = \rho(\lambda)$ is a constant. In this case, the Landsat radiance is given by

$$L(\lambda,e) = L_n(\lambda)\cos i \qquad (1)$$

where L_n is constant equal to $A(\lambda)\,\rho(\lambda)$. We term L_n the effective normal response that would be measured when $i = e = 0°$.

Several authors, however, have reported a dependence of reflected light on sensor and illumination geometry that departs from this relationship (Kriebel, 1978; Duggin, 1977; Smith and Oliver,

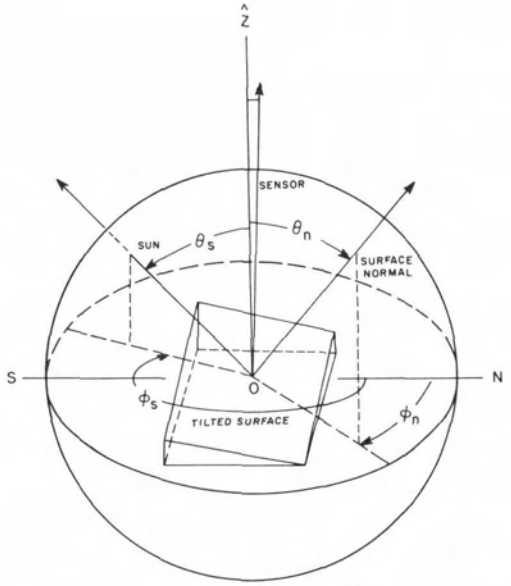

FIG. 1. Diagram of geometric relationships between sun and sensor positions.

1974; Proctor *et al.*, 1972; Stewart, 1971; Coulson, 1966; and Monteith and Szeicz, 1961).

A more general relationship is given by an empirical photometric function proposed by Minnaert (1941). In this case, the bidirectional reflectance factor is given by

$$\rho(\lambda,e,i) = \rho(\lambda) \cos^{k(\lambda)-1} i \cos^{k(\lambda)-1} e$$

and the satellite radiance is given by:

$$L(\lambda,e) = L_n(\lambda) \cos^{k(\lambda)} i \cos^{k(\lambda)-1} e \qquad (2)$$

where k is the Minnaert constant. Generally, k also varies with phase angle, α, defined as the angle between the sensor and the illumination source. For Landsat data, however, the phase angle is considered constant. The Minnaert constant, k, describes the type of scattering dependence and is related to surface roughness. If k = 1, a Lambertian surface is defined and Equation 2 reduces to Equation 1. Low values of k imply a porous surface which exhibits asymmetrical diffuse scattering (Young and Collins, 1971). Values of k unequal to 1.0 imply a combination of diffuse and specular scattering.

This Minnaert function has received widespread use in the field of astrophysics to determine the surface characteristics of planetary bodies (Veverka *et al.*, 1978; Binder and Jones, 1972; Young and Collins, 1971; and Hapke and Van Horn, 1963, as examples). Its application to terrestrial remote sensing, however, has been limited (Gillespie and Kahle, 1977).

A strong test of the Lambertian assumption can be made by first linearizing Equation 2 and then obtaining the regression value for k. That is,

$$L \cos e = L_n \cos^k i \cos^k e$$

and

$$\log (L \cos e) = \log L_n + k \log (\cos i \cos e).$$

Letting y = log (L cos e), the response variable,
x = log (cos i cos e), the independent variable, and
b = log (L_n),

we obtain the linear form $y = kx + b$.

A t-test of significance can then be made for the hypothesis that the slope coefficient, k, is equal to 1.0.

Equations 1 and 2 may also be inverted to develop backward radiance correction transformations for topographic slope and aspect. That is, using the Lambertian assumption:

$$L_n = L/\cos i \qquad (3)$$

Using the Minnaert relationship:

$$L_n = (L \cos e) / (\cos^k i \cos^k e) \qquad (4)$$

In this study we first evaluate the Minnaert k coefficient by regression analysis and then apply both correction procedures (Equations 3 and 4) to evaluate their likely effect on image classification.

Data Reduction and Analysis

Figure 2 is a reduced orthophotograph of the study site used in this analysis. The study area is located in the Front Range of the Rocky Moun-

FIG. 2. Horsetooth Reservoir, Colorado study area.

tains about 5 miles (8 km) west of Fort Collins, Colorado. The dominant features include sedimentary rock formations uplifted into hogbacks in the east, high steep mountains of metamorphic and igneous rock to the west, and Horsetooth Reservoir located in the east-central portion of the study site. Site elevations range from about 4500 ft (1370 m) to 7400 ft (2255 m).

Vegetative cover in the mountains is primarily ponderosa pine (*Pinus ponderosa*) with understory and open areas consisting of grasses and shrubs. There are also lesser areas of some riparian vegetation. Horsetooth Reservoir occupies approximately 2.5×10^3 acres (1.0×10^3 ha) and lies in a north-south direction across the study site.

A 15 August 1973 Landsat image of the study site was obtained for radiometric analysis. The solar zenith angle at image acquisition was 37 degrees; solar azimuth was 114 degrees. The Landsat image was first geometrically corrected to a scale of 1:24,000 using a nearest-neighbor algorithm (Anuta, 1973). Grey level printouts of each multispectral band were then overlaid on a 1:24,000 quadrangle map of the study site published by the United States Geological Survey in 1962. A 1970 quadrangle centered orthophoto for the study site was also available for comparison. Image to ground registration was improved locally by comparing image grey tones for such distinctive morphological features as stream patterns, rock outcroppings, and water bodies to the topographic map. Once registration between the computer grey level printouts and the topographic map was obtained, a grid-cell overlay with cell dimensions approximately equal to the digital Landsat map was constructed.

Selection of pixels representing ponderosa pine was accomplished by first overlaying a 1:24,000 scale ecosystem map prepared by the Colorado State Forest Service in 1974 and delineating areas classed as ponderosa pine. The criteria used for ponderosa pine included areas greater than 5 acres with a crown closure of ponderosa pine greater than 50 percent (Lynch, 1974). Based on this overlay, 364 pixels were initially selected for analysis. Since this ecosystem classification included open areas of shrub understory within the ponderosa pine class, further analysis was required to select pixels which only included dense ponderosa pine. This was accomplished by overlaying the quadrangle centered orthophoto, the topographic map, and the Landsat grey maps. Pixels were selected from areas where dense ponderosa pine occurred and that were circumscribed by pixels with similar radiance values. In addition, these pixels were selected from the center of areas of similar slope and aspect as determined from the topographic map. The procedure of selecting only pixels of dense ponderosa pine evident from the orthophoto and the Landsat grey maps and located with areas of relatively constant slope and aspect significantly reduced the possibility of errors caused by slight misregistration of the various overlays and the Landsat grey maps.

A subset of 76 pixels was ultimately selected for final analysis. The topographic slope, θ_n, and aspect, ϕ_n, for each of the pixels were determined from the topographic map and merged with the respective Landsat digital counts for MSS bands 4, 5, 6, and 7. For our data set, effective incidence angles ranged from 35 to 75 degrees, exitance angles ranged from 10 to 45 degrees, and aspects ranged within ±50 degrees of north.

Figure 3 shows the scatter of the data transformed by linearizing Equation 2 for a visible spectral band, MSS 5, and an infrared band, MSS 7, as displayed in a Minnaert plot. A regression equation of the linearized version of the Minnaert function was computed for each wavelength band. The results are shown in Table 1. In all cases the Minnaert constant, k, or the slope of the regression line, is significantly less than 1.0 at the 95 percent confidence level.

We, therefore, conclude that for the range of incidence angles, 30 to 80 degrees, and exitance angles, 10 to 45 degrees, studied, the Lambertian assumption for the Landsat response from ponderosa pine is invalid.

For comparison, a regression equation for the 76 pixels utilizing the simple, but incorrect, Lambertian function was also computed. As expected, significantly less of the Landsat variation is explained by this procedure than by employing the Minnaert function.

Discussion and Recommendations

Figure 4 shows the Landsat response as corrected by the transformation given by Equation 4

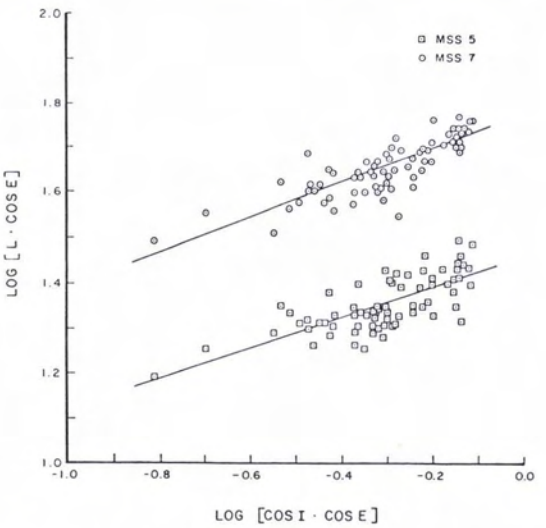

Fig. 3. Minnaert plots of Landsat MSS Ponderosa pine data.

TABLE 1. MINNAERT REGRESSION RELATIONSHIPS FOR EACH LANDSAT MSS CHANNEL

Landsat Channel	Minnaert Constant, k	t-value ($k = 1$)	R^2
4	0.26	35.2**	0.68
5	0.33	20.9**	0.58
6	0.38	22.1**	0.71
7	0.37	21.7**	0.68

** Significant at the 95 percent confidence level with 75 degrees of freedom.

versus the cosine of the incidence angle for MSS bands 5 and 7. It is evident that this correction procedure does lead to a level response versus the varying effective solar incidence angle. Consequently, we have appeared to reduce this extrinsic source of radiance variation for these sample observations.

In contrast, Figure 5 shows the effect of applying the correction transformation of Equation 3. It is evident that, in reality, this procedure introduces *more* variation into the data at large incidence angles. Consequently, it would be better to leave the data uncorrected than apply this transformation which is based on an assumed, but incorrect, hypothesis; in this case, the Lambertian assumption.

We have demonstrated that, for incidence angles between 30 and 80 degrees and for exitance angles between 10 and 45 degrees, the Landsat response from ponderosa pine (*Pinus ponderosa*) does not follow the Lambertian law. Are there ranges of exitance or incidence angles for which the Lambertian assumption is more nearly valid? A closer examination of Figure 5 indicates that if $\cos i$ is greater than 0.7, i.e., if the incidence angle is less than 45 degrees, then a more level response results.

To examine this question in more detail, we ratio the Lambertian-expected radiance, Equation 1, to the Minnaert-expected radiance, Equation 2, and obtain

$$\text{Ratio, } R, = \cos^{1-k} i \cos^{1-k} e.$$

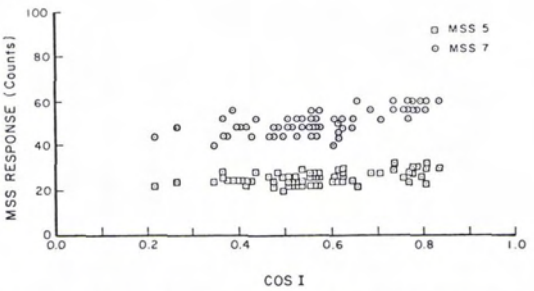

FIG. 4. Minnaert corrected Landsat MSS data of ponderosa pine versus cosine of effective incidence angle (cos I).

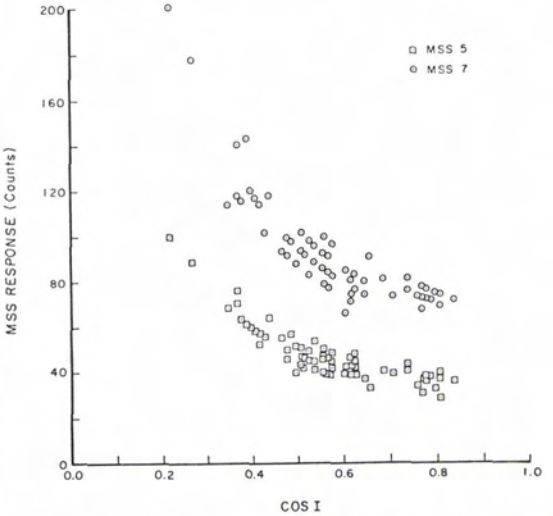

FIG. 5. Lambertian corrected Landsat MSS data of ponderosa pine versus cosine of effective incidence angle (cos I).

Or, setting $k = 0.37$, the value we obtained for MSS band 7, we obtain

$$R = \cos^{0.63} i \cos^{0.63} e.$$

Figure 6 shows the contours of constant value for this ratio plotted versus incidence, i, and exitance, e, angles. These curves indicate that, for a given ratio, a subregion of restricted values for i and e can be defined such that a more nearly Lambertian response would be expected. As an example, we performed a data cut on our 76 observations and selected only those pixels with slopes less than 25 degrees and incidence angles less than 45 de-

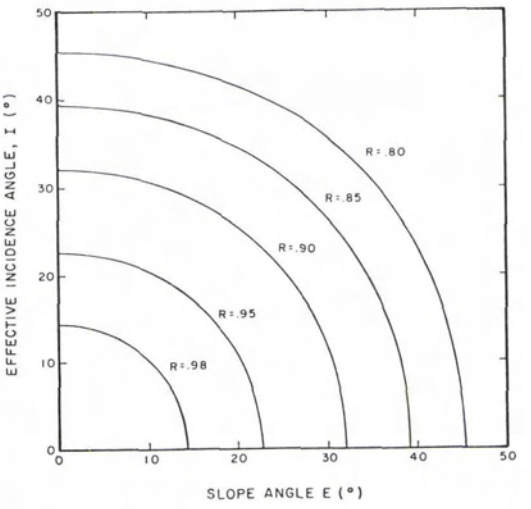

FIG. 6. Ratio of Lambertian-expected radiance to Minnaert-expected radiance. Contours of constant ratio value are shown.

grees, corresponding to a ratio generally greater than 0.8 from Figure 6. Eighteen sample points satisfied these criteria. We obtained a k value for MSS band 7 of 0.9 ± 0.2. The estimated k value for MSS band 5 was 0.6 ± 0.5. Thus, as predicted, for restricted ranges of incidence and exitance angles, the Lambertian assumption is more nearly satisfied.

As an application of our Minnaert-derived radiance function, we address the question of topographic-induced Landsat radiance variations versus surface cover variations. It is well-known that topographic influences are most easily seen in imagery collected at low sun elevation angles. Conversely, at high sun angles and small slopes the scene radiance is dominated by surface cover variations. We can estimate these effects by following the method outlined by Horn and Bachman (1978). If surface slopes (exitance angles) range between 0° and e, then an extreme range of incidence angles, i, for a given solar elevation angle, ψ_s, will be defined by

$$\cos(e - 90 - \psi_s) < \cos i < \cos(e + 90 - \psi_s).$$

Letting the range of absolute surface reflectance, ρ, be defined from ρ_1 to ρ_2, we obtain the following expression which defines the critical slope value, e, for a given solar inclination angle, ψ_s, where the maximum reflectance differences are equal:

$$\rho_1 \cos^k(e - 90 - \psi_s) \cos^k e = \rho_2 \cos^k(e + 90 - \psi_s) \cos^k e.$$

This expression can be reduced to

$$\tan e_c = \frac{\rho_1^{1/k} - \rho_2^{1/k}}{\rho_1^{1/k} + \rho_2^{1/k}} \tan \psi_s$$

where e_c is the critical slope angle for a given solar elevation angle, ψ_s, above which topography will affect the scene radiance more than the differences in absolute reflectances, ρ_1, ρ_2.

In Figure 7 we plot the critical slope angle versus solar elevation angle for scene elements whose reflectances differ by 10 percent, i.e., $\rho_1 = 1.1\ \rho_2$, and by 100 percent. The k value for MSS band 7 was employed. In both cases, the larger the solar elevation angle, the larger the critical slope angle. That is, at high solar positions, the Landsat radiance is sensitive to surface reflectance differences over a wider range of topographic slopes. In our experiment, the solar elevation angle was 57 degrees. Thus, we predict that we should be able to detect surface reflectance differences of 10 percent only for pixels whose slopes are less than 12 degrees. Similarly, in order to differentiate reflectance differences of 100 percent, the surface cover must be on slopes less than 49 degrees.

In conclusion, we have demonstrated that the Lambertian assumption is not strictly valid for our ponderosa pine Landsat data. However, our results indicate that the Lambertian approximation is more nearly valid if suitable restrictions are imposed on the range of incidence or exitance angles. Since our ponderosa pine samples occurred on slopes with a primarily northerly aspect, it may be useful to perform the Minnaert analysis on data acquired over a wider range of aspects. Further research is also required to address the suitability of the Lambertian assumption for surface cover types other than the ponderosa pine samples examined here. For example, how does the Minnaert constant, k, vary with surface cover type? Further study is also required in order to evaluate the use of such expressions as Equation 4 for scene normalization.

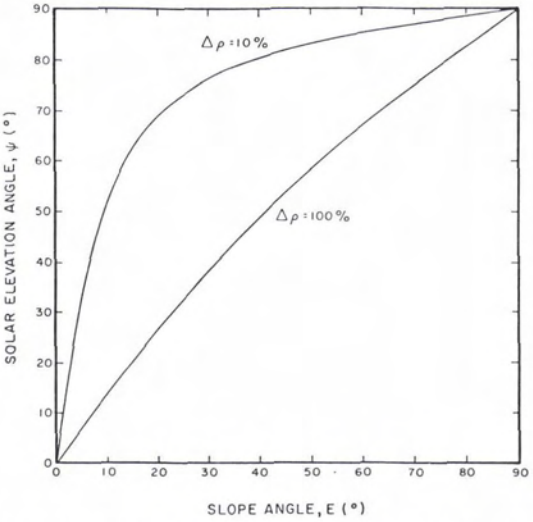

FIG. 7. Critical slope angle versus critical solar elevation angle for Minnaert Terrain elements with surface reflectance differences of 10 percent and 100 percent.

ACKNOWLEDGMENTS

The research described in this paper was supported by the U.S. Forest Service under Cooperative Agreement CA-16-741, "Signature Studies for Natural Resource Inventory." Mr. Robert Dana of the Rocky Mountain Forest and Range Experiment Station was technical monitor of the project.

Mr. Tzeu Lie Lin received the Master of Science degree from Colorado State University, in part, for work related to this project.

REFERENCES

Anuta, P., 1973. *Geometric Correction of ERTS-1 Digital Multispectral Scanner Data.* LARS Information Note: 103073. Purdue University, West Lafayette, Indiana. 23 p.

Binder, A., and J. Jones, 1972. Spectrophotometric Studies of the Photometric Function, Composition and Distribution of the Surface Materials of Mars. *J. of Geophys. Res.* 77:3005-3020.

Coulson, K. L., 1966. Effects of Reflection Properties of Natural Surfaces in Aerial Reconnaissance. *Applied Optics* 5:905-917.

Crane, R. B., 1971. Preprocessing Techniques to Reduce Atmospheric and Sensor Variability in Multispectral Scanner Data. *Proc. of the 7th Int. Symp. on Remote Sensing of Environment*, Ann Arbor, Michigan, pp. 1345-1355.

Duggin, M. J., 1977. Likely Effects of Solar Elevation of the Quantification and Changes in Vegetation with Maturity Using Sequential Landsat Imagery. *Applied Optics* 16:521-523.

Gillespie, A. R., and A. B. Kahle, 1977. Construction and Interpretation of a Digital Thermal Inertia Image. *Photo. Eng. Rem. Sens.* 43(8):983-999.

Hapke, B., and H. Van Horn, 1963. Photometric Studies of Complex Surfaces with Applications to the Moon. *J. of Geophys. Res.* 68(15):4545-4570.

Hart, T., 1978. *Reduction of Topographic Shadow Effects in Landsat by Division of Mean Brightness.* M. S. Thesis, Earth Resources Dept., Colorado State University, Fort Collins, Colorado. 80 p.

Hoffer, R., 1974. *Natural Resources Mapping in Mountainous Terrain by Computer Analysis of ERTS-1 Satellite Data.* LARS/Purdue University, West Lafayette, Indiana. 124 p.

Horn, B. K. P., and B. Bachman, 1978. Using Synthetic Images to Register Real Images with Surface Models. *Comm. ACM* 21:914-924.

Kriebel, K. T., 1978. Measured Spectral Bidirectional Reflection Properties of Four Vegetated Surfaces. *Applied Optics* 17(2):253-258.

Lynch, D. L., 1974. *An Ecosystem Guide for Mountain Land Planning. Level I.* Colorado State Forest Service, Colorado State University, Fort Collins, Colorado. 94 p.

Minnaert, M., 1941. The Reciprocity Principle in Lunar Photometry. *Astrophys. J.* 93:403-410.

Monteith, J. L., and G. Szeicz, 1961. The Radiation Balance of Bare Soil and Vegetation. *Quart. J.R. Met. Soc.* 87:159-170.

Oliver, R. E., J. K. Berry, and J. A. Smith, 1975. A Portable Instrument for Measuring Apparent Directional Reflectance. *Opt. Engineering* 14:244-247.

Proctor, J. T. A., W. J. Kyle, and J. A. Davies. 1972. The Radiation Balance of an Apple Tree. *Can. J. Bot.* 50(8):1731-1740.

Smith, J. A., and R. E. Oliver, 1974. Effects of Changing Canopy Directional Reflectance on Feature Selection. *Applied Optics* 13(7):1599-1604.

Stewart, J. B., 1971. The Albedo of a Pine Forest. *Quart. J.R. Met. Soc.* 97:561-564.

Struve, H., W. Graham, and H. West, 1977. *Acquisition of Terrain Information Using Landsat Multispectral Data.* Report 1 of series, Technical report M-77-2, Mobility and Environ. System Laboratory U.S. Army Engineering Waterway Experiment Station, Vicksburg, MS 39180, 50 p.

Veverka, J., 1972. Effects of Surface Roughness on the Photometric Properties of Mars. *ICARUS* 16:281-288.

Vincent, R. K., 1973. Spectral Ratio Imaging Methods for Geological Remote Sensing from Aircraft and Satellites. *Proc. of Symp. on Management and Utilization of Remotely Sensed Data*, American Society of Photogrammetry, Sioux Falls, SD, October, pp. 377-397.

Young, A. T., and S. A. Collins, 1971. Photometric Properties of the Mariner Cameras and of Selected Regions of Mars. *J. of Geophys. Res.* 76(2):432-437.

(Received 10 January 1979; revised and accepted 28 March 1980)

Colloquium
on the Application of the Next Generation of Earth Resource Satellites

Montréal, Canada
25-26 November 1980

The colloquium is jointly sponsored by the Ministère de l'Energie et des Ressources du Québec and the Canada Centre for Remote Sensing. The objective of the colloquium is to determine as precisely as possible the format and way of using the data products from the next generation of Earth resource satellites, namely Landsat D and SPOT.

The colloquium will be based on a program of simulated data products. Certain application areas will be selected for scrutiny by resource persons. The meeting will accommodate presentation of results followed by critical discussions.

For further information please contact

Keith P. B. Thomson
Canada Centre for Remote Sensing
2464 Sheffield Road
Ottawa, Canada K1A 0Y7
Tel. (613) 995-1210